Circulation Model for Absorption and Dispersion in Cocurrent Bubble Columns

Richard G. Rice, Nicholas W. Geary, and Louis F. Burns
Chemical Engineering Dept., Louisiana State University, Baton Rouge, LA 70803

Liquid circulation and a finite entrance zone are accounted for in modeling gas absorption into cocurrent flows of pure oxygen and CMC solutions. The new models lead to a Taylor-like correction factor to account for circulation in both absorption and transient dispersion experiments. Steady-state experiments for viscosities of 1, 12, 25 and 50 mPa·s were conducted by measuring dissolved gas concentration profiles along the column axis. Liquid mixing experiments were performed using the transient acid-base neutralization method, leading to measured values of axial dispersion coefficients which depended on viscosity to the power 0.75. Measurements suggest that circulation was minuscule owing to uniform gas injection by Flexisparger in the present column.

Introduction

Bubble columns are widely used in the process and biotechnology industries owing to their simplicity of construction and effectiveness in mass transfer. Although simple to build and operate, they nonetheless pose difficult design problems, since behavior of such gas-liquid emulsions is surprisingly complicated and unpredictable. Only recently (Clark et al., 1987; Rice and Geary, 1990; Geary and Rice, 1992) have workers come to grips with the phenomenon of circulation in bubble columns from the point of view of first principles. It now seems clear (Geary and Rice, 1992) that circulation is buoyancy-induced and arises from radial nonuniformity of gas voidage. Moreover, it now appears the controlling mode of turbulence arises in different ways, depending on column size. Thus, Geary and Rice (1992) suggest turbulent eddy size is proportional to bubble size for small columns, and for larger columns it depends on column diameter. It was concluded that, even for low voidage conditions, circulation always exists (to a smaller extent as voidage uniformity is maintained) owing to a narrow, bubble-free region near the wall.

These observations have far-reaching effects on scale-up and could possibly influence predictions based on the standard plug-flow model for mass transfer.

In this article, we consider a new model for bubble columns which accounts for the entrance zone (where mass transfer is large) and also for effects arising from uniform liquid circulation. One outcome of the model leads to a forecast of a Taylor-type axial dispersion coefficient which is shown to depend on circulation velocities and the radial exchange of material between upflowing and downflowing regions. Another interesting result is the way interphase mass transfer is affected by the circulation, relative to the noncirculating, plug-flow model. We compare the asymptotic form of the model with experiments of two types:

1. Measurement of steady-state dissolved gas composition along the column axis.
2. Measurement of dispersion in a transient experiments using acid-base neutralization.

Steady-State Model for Gas Absorption with Circulation

To account for circulation, we apportion the column proper into upflowing and downflowing zones as shown in Figure 1. These are connected to an entrance zone, covering the full-column cross-section, which is modeled as an ideal CSTR. The height of the entrance zone can vary and will be deduced based on independent acid-base experiments. Liquid carrying a dissolved gas composition C_o enters the column at volume flow Q_o. The dissolved gas composition at the entrance zone (CSTR) is denoted as C, which is taken equal to be $C_u(0)$ for ideal mixing conditions. Upflow, downflow gas compositions are denoted by $C_u(z)$ and $C_d(z)$, respectively. Conservation for liquid flows requires:

Correspondence concerning this article can be addressed to R. G. Rice.
Present address of N. W. Geary: Procter and Gamble Co., Cincinnati, OH 45241.

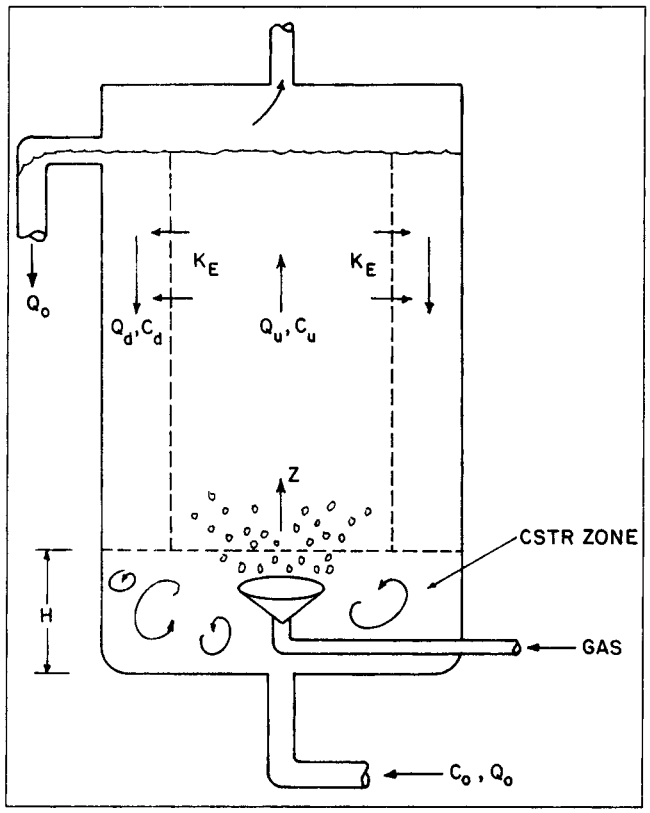

Figure 1. Circulating bubble column with entrance CSTR zone.

$$Q_u = Q_d + Q_o \tag{1}$$

and the material balances for the counterflowing liquid zones are taken to be:

$$Q_u \frac{dC_u}{dz} = k_c a A_u (C^* - C_u) - K_E (C_u - C_d) \tag{2}$$

$$-Q_d \frac{dC_d}{dz} = k_c a A_d (C^* - C_d) + K_E (C_u - C_d) \tag{3}$$

where A_d and A_u are downflow and upflow cross-sectional areas, respectively, and K_E represents the product of radial exchange coefficient and a characteristic area per unit height separating the two zones. Thus, $K_E(C_u - C_d)$ represents the exchange rate between zones, which is a rate proportional to the radial flux component of eddy diffusion. Recent experiments by Lubbert and Larson (1990) suggest that radial mixing is rather more diffusion-like than axial mixing, which has properties that combine diffusion and convection. They reach these conclusions, using heat tracers to assess dispersion over small distances, by correlating the time variation of standard deviation, $\sigma(t)$. Thus, a "source" spreading only by diffusion has $\sigma \propto \sqrt{t}$, or spreading by convection they give $\sigma \propto t$, and by isotropic turbulence they suggest $\sigma \propto t^{3/2}$. Their experimental measurements gave for axial mixing $\sigma_z \propto t^{0.8}$ and for radial mixing $\sigma_r \propto t^{0.59}$, the latter very nearly diffusion-like in behavior. The intermediate nature they found for axial mixing suggests that both diffusive and convective modes are acting. As we shall show, the present analysis leads to an effective axial dispersion coefficient which takes a form very similar to so-called Taylor diffusion, combining two terms: eddy diffusivity plus a convective Taylor-like diffusivity.

To solve Eqs. 2 and 3, we need to know how the flow areas change in each section. This is determined from the transition point, δ, which is the dimensionless radial position where positive upflow velocity charges to downflow, so it is the point of zero velocity. Recent calculations (Geary, 1991; Geary and Rice, 1992) indicate for a rather wide range of conditions, the dimensionless transition point is approximately:

$$\delta \simeq 1/\sqrt{2} \tag{4}$$

which of course implies $A_u = A_d = A$, so upflow and downflow areas are taken henceforth to be equal.

By making independent variables dimensionless, Eqs. 2 and 3 become:

$$q_u \frac{d\theta_U}{d\zeta} + \theta_u = \alpha \theta_d \tag{5}$$

$$-q_d \frac{d\theta_d}{d\zeta} + \theta_d = \alpha \theta_u \tag{6}$$

The dimensionless coefficient $\alpha = K_E/(k_c aA + K_E)$ is a measure of the importance of the exchange coefficient K_E, in relation to the interfacial mass-transfer coefficient, expressed as $k_c a \cdot A$.

The solutions to the equation can be effected quite easily using Heaviside operators, $D = d/d\zeta$:

$$[q_u D + 1]\theta_u = \alpha \theta_d \tag{7}$$

$$[-q_d D + 1]\theta_d = \alpha \theta_u \tag{8}$$

By operating on Eq. 7, using the operator from Eq. 8, we see:

$$[-q_d D + 1][q_u D + 1]\theta_u = \alpha[-q_d D + 1]\theta_d = \alpha^2 \theta_u \tag{9}$$

This leads to:

$$[-q_d q_u D^2 + (q_u - q_d)D + (1 - \alpha^2)]\theta_u = 0 \tag{10}$$

An identical expression for θ_d is obtained by applying the operator from Eq. 7 to Eq. 8. We take note that from Eq. 1:

$$q_u - q_d = \frac{Q_u - Q_d}{Q_o} = \frac{Q_o}{Q_o} = 1 \tag{11}$$

hence we have for either θ_u or θ_d:

$$-q_d q_u \frac{d^2\theta}{d\zeta} + \frac{d\theta}{d\zeta} + (1 - \alpha^2)\theta = 0 \tag{12}$$

The characteristic roots for either θ_u or θ_d are obtained from:

$$-q_d q_u r^2 + r + (1 - \alpha^2) = 0 \tag{13}$$

hence

$$r_{\pm 1}=\frac{1}{2q_dq_u}\left[1\pm\sqrt{1+4q_dq_u(1-\alpha^2)}\right] \tag{14}$$

so solutions can be written,

$$\theta_u=K_u\exp(\zeta r_{-1})+L_u\exp(\zeta r_{+1}) \tag{15}$$

$$\theta_d=K_d\exp(\zeta r_{-1})+L_d\exp(\zeta r_{+1}) \tag{16}$$

In the limit as $\zeta\to\infty$, we require $\theta_u\to 0$, and $\theta_d\to 0$, so we set $L_u=L_d=0$.

Now, K_u and K_d are not linearly independent constants of integration, which can be seen by inserting Eqs. 15 and 16 into the defining relations, Eqs. 5 and 6, to see:

$$K_u=\frac{\alpha}{q_ur_{-1}+1}K_d \tag{17}$$

so that the solutions with a single arbitrary constant are:

$$\theta_u=\left(\frac{\alpha}{q_ur_{-1}+1}\right)K_d\exp(\zeta r_{-1}) \tag{18}$$

$$\theta_d=K_d\exp(\zeta r_{-1}) \tag{19}$$

Thus, we need only an entrance condition to evaluate K_d.

Entrance Condition and Final Solution

Inspecting Figure 1, we arrive at the following material balance for the CSTR zone at the column entrance:

$$Q_dC_d(0)=[Q_u+k_c^*aV]C_u(0)-Q_oC_o-k_c^*aVC^* \tag{20}$$

where k_c^*a denotes the high rate mass-transfer coefficient in the entrance region, where it is expected $k_c^*a>k_ca$. In terms of θ_u, θ_d, the CSTR balance is:

$$q_d\theta_d(0)=\left(q_u+\frac{k_c^*aV}{Q_o}\right)\theta_u(0)+(C^*-C_o) \tag{21}$$

Inserting Eqs. 18 and 19 into this yields for K_d:

$$K_d=\frac{(C^*-C_o)}{q_d-\left[q_u+\dfrac{k_c^*aV}{Q_o}\right]\left(\dfrac{\alpha}{q_ur_{-1}+1}\right)} \tag{22}$$

The complete solutions can now be written:

$$\frac{\theta_u}{(C^*-C_o)}=\frac{\alpha\exp\left[\dfrac{\zeta}{2q_d\cdot q_u}\left(1-\sqrt{1+4q_d\cdot q_u(1-\alpha^2)}\right)\right]}{q_d(q_ur_{-1}+1)-\left(q_u+\dfrac{k_c^*aV}{Q_o}\right)\alpha} \tag{23}$$

$$\frac{\theta_d}{(C^*-C_o)}=\frac{(q_ur_{-1}+1)\exp\left[\dfrac{\zeta}{2q_d\cdot q_u}\left(1-\sqrt{1+4q_d\cdot q_u(1-\alpha^2)}\right)\right]}{q_d(q_ur_{-1}+1)-\left(q_u+\dfrac{k_c^*aV}{Q_o}\right)\alpha} \tag{24}$$

Dispersion Relation

Equation 12 can be written in dimensional form and we thereby deduce an effective value for Dispersion coefficient (exclusive of the eddy diffusivity component); thus, by inspection we see:

$$\frac{Q_dQ_ud^2C_u}{A^2(k_ca+K_E/A)dz^2}-\frac{Q_o}{A}\frac{dC_u}{dz}+(1-\alpha^2)(k_ca+K_E/A)(C^*-C_u)=0 \tag{25}$$

The total cross-sectional area is $A_o=2A$, so if we define superficial velocity of injected liquid in the usual way as $U_o=Q_o/A_o$ then we can write Eq. 25 as:

$$D_e\frac{d^2C_u}{dz^2}-2U_o\frac{dC_u}{dz}+K_La(C^*-C_u)=0 \tag{26}$$

where we have defined effective dispersion and transport coefficients as:

$$D_e=\frac{Q_dQ_u}{A^2(k_ca+K_E/A)}=\frac{V_d\cdot V_u}{(k_ca+K_E/A)} \tag{27}$$

$$K_La=(1-\alpha^2)(k_ca+K_E/A)=k_ca(1+\alpha) \tag{28}$$

Note that D_e has a structure identical to Taylor Diffusion, in the sense we have a form with squared velocity divided by diffusivity. Here, K_E is proportional to eddy diffusivity in the radial direction, and it also possesses units of diffusivity (length^2/time).

The characteristic roots for Eq. 26 must be identical to those from Eq. 13. Thus the argument of the exponential solutions must be identical, so

$$\frac{zU_o}{D_e}\left[1-\sqrt{\frac{1+K_LaD_e}{U_o^2}}\right]=\frac{\zeta}{2q_dq_u}\left[1-\sqrt{1+4q_dq_u(1-\alpha^2)}\right] \tag{29}$$

Thus, the final solution can be written in terms of D_e and K_La:

$$\frac{C^*-C_u}{C^*-C_o}=\frac{\alpha\exp\left[z\dfrac{U_o}{D_e}\left(1-\sqrt{1+\dfrac{K_LaD_e}{U_o^2}}\right)\right]}{\alpha\left[1+\dfrac{k_c^*aV}{Q_o}\right]+(\alpha-1)\dfrac{Q_d}{Q_o}+\dfrac{1}{2}\left[-1+\sqrt{1+\dfrac{K_LaD_e}{U_o^2}}\right]} \tag{30}$$

$$\frac{C^* - C_d}{C^* - C_o} = \frac{\left[1 + 2\left(\frac{Q_d}{Q_o}\right) - \sqrt{1 + \frac{K_L a D_e}{U_o^2}}\right] \exp\left[z \frac{U_o}{D_e}\left(1 - \sqrt{1 + \frac{K_L a D_e}{U_o^2}}\right)\right]}{\left(2\frac{Q_d}{Q_o}\right)\left\{\alpha\left[1 + \frac{k_c^* a V}{Q_o}\right] + (\alpha - 1)\frac{Q_d}{Q_o} + \frac{1}{2}\left[-1 + \sqrt{1 + \frac{K_L a D_e}{U_o^2}}\right]\right\}} \quad (31)$$

Asymptotic Behavior

It is useful to inspect the limits on the derived solutions for the circulation model, in particular, to find when a simple plug-flow model is suitable. We consider two extremes: $Q_d \sim 0$, and $K_E \to \infty$. These are practical and observable cases, corresponding to small backflow and large radial mixing, respectively.

Case when $Q_d \sim 0$; backflow tending small

Under this circumstance, Eq. 27 shows the dispersion coefficient (D_e) becomes diminishingly small, so we can write $\sqrt{1 + K_L a D_e / U_o^2} \sim 1 + 1/2 \quad K_L a D_e / U_o^2$ and since $K_L a = k_c a(1 + \alpha)$:

$$\frac{C^* - C_u(z)}{C^* - C_o} \simeq \frac{\exp\left(-\frac{z k_c a(1+\alpha)}{2U_o}\right)}{1 + \frac{k_c^* a V}{Q_o}} \quad (32)$$

$$\frac{C^* - C_d(z)}{C^* - C_o} \simeq \frac{\alpha \exp\left(-\frac{z k_c a(1+\alpha)}{2U_o}\right)}{\left(1 + \frac{k_c^* a V}{Q_o}\right)} \quad (33)$$

Moreover, if radial mixing is large ($\alpha \sim 1$), this reduces to the plug-flow model, and $C_u \sim C_d$.

Case when $K_E \to \infty$ ($\alpha \sim 1$); large radial mixing

When mixing in the radial direction is large, concentration differences between C_u and C_d cannot be sustained, and in the limit: $K_L a \sim 2k_c a$ and $D_e \sim 0$, which leads to the asymptotic result:

$$\frac{C^* - C_u}{C^* - C_o} \simeq \frac{\exp\left(-\frac{z k_c a}{U_o}\right)}{1 + \frac{k_c^* a V}{Q_o}} \quad (34)$$

$$\frac{C^* - C_d}{C^* - C_o} \simeq \frac{\exp\left(-\frac{z k_c a}{U_o}\right)}{1 + \frac{k_c^* a V}{Q_o}} \quad (35)$$

which are formally identical to the plug flow (nonrecirculating model), no matter how much circulation exists. Moreover, we see that $C_u \sim C_d$, as required for a plug model. This plug-flow result is different from that obtained heretofore in literature, since it accounts for enhanced transport in the entrance region. This correctly shows that the intercept at $z = 0$ is not unity (the case for standard plug-flow models).

The detailed fluid mechanics for recent circulation models put forth by Geary and Rice (1990, 1992) will always sustain a small backflow (finite circulation) owing to the structure of the model, which postulated that there always exists a clear, bubble-free layer near the wall, hence there must always exist a finite buoyancy driving force, however small. Hence, no matter how uniformly the gas is distributed over the column cross-section, this model predicts there will always exist a small, but finite level of circulation in all bubble columns. This is illustrated quite strikingly in a recent article (Geary and Rice, 1992) where the large column data of Kojima et al. (1980) was studied, and in spite of a very flat voidage profile, it was shown that significant circulation (60 cm/s at the centerline) could still arise from the very slight density gradient near the wall. Nonetheless, the present analysis shows that this circumstance may not complicate the design exercise, since when K_E is large (large eddy mixing), the system behaves like a noncirculating plug-flow contactor. For practical purposes, circulation appears to have little untoward effect, except possibly for highly viscous systems. Circulation in viscous systems can be large, but eddy diffusivity is damped so that the exchange coefficient K_E may be small, which suggests $\alpha < 1$. Under such conditions, transport coefficients may be significantly different from those determined from a plug-flow model.

Before we can apply actual steady-state data to the model, we shall need to independently find the height of the entrance (CSTR) zone, since otherwise we would need to contend with a product of two unknown parameters, that is, $k_c^* a V / Q_o$. We can find V/Q_o or H/U_o by independent means using acid-base neutralization experiments (Rice and Littlefield, 1987; Rice et al., 1990; Geary, 1991). We discuss the basis for the acid-base technique next.

Transient Dispersion Model

In addition to steady-state absorption experiments, a relatively new technique, acid-base neutralization, was used to assess effective dispersion coefficient. This transient method also provided good estimates of the height of the inlet CSTR zone (H). This height is needed in order to deduce $k_c^* a$ in the steady-state absorption model.

The liquid-based acid-base technique was apparently first used to assess dispersion coefficient by Rice and Littlefield

(1987). The method yielded up a bonus by clearly showing the sensitivity to the importance of column verticality. Thus, even miniscule tilt (0.25°) produced startling changes in flow patterns, relative to the uniformly noncirculating pattern obtained for perfect verticality. Later, Rice, Barbe and Geary (1990) improved the parameter estimation technique so that accurate estimates of CSTR height could be obtained.

Before discussing this technique, we next wish to show that, even with circulation present, tracers injected into batch bubble columns are expected to behave according to a form of Fick's second law, henceforth called Fickian-like.

Modeling Dispersion with Circulation

The locally varying interstitial velocity, $U_c(r)$, according to our recent theories (Rice and Geary, 1990; Geary and Rice, 1992) takes an elementary integral form, which is a bit tedious to apply to the convective diffusion equation. Nonetheless for the sake of completeness, we write the axial velocity model to describe transient movement of an injection tracer as:

$$\epsilon_l(r)\frac{\partial C}{\partial t}+\epsilon_l(r)U_c(r)\frac{\partial C}{\partial r} \tag{36}$$

$$=\frac{1}{r}\frac{\partial}{\partial r}\left(D_r^*\epsilon_l(r)r\frac{\partial C}{\partial r}\right)+D_z^*\epsilon_l(r)\frac{\partial^2 C}{\partial z^2} \tag{36}$$

where U_c is positive for upflow, negative for downflow. Here, $\epsilon_l(r)$ denotes the locally varying volume fraction liquid [which is $1-\epsilon(r)$, where $\epsilon(r)$ = gas fraction] and D_r^*, D_z^* are the directional values of eddy diffusivity. If the usual power-law model is used to model local gas voidage, it is possible to integrate the above relation for certain special cases [for example, highly viscous solutions, since it was shown by Rice and Geary (1990) for this case that U_c takes a power series form].

However, our purposes here are to elucidate the essential effects arising from circulation, so a simplified model is needed. As in the steady-case, we model circulation as plug-flow in each respective direction, using an average liquid fraction $\bar{\epsilon}_l$. We account for radial exchange between upflowing and downflowing regions in a manner exactly like the steady-state absorption model, by introducing an exchange coefficient. The following approach was apparently first used for an "entrainment" model (Rietema, 1982) and was also derived for a circulating model, as in the present case, by Wilkinson (1991) to study the effect of high pressure on mixing.

We shall need two transport equations to separately describe upflow and downflow regions:

$$\frac{\partial C_u}{\partial t}+U_u\frac{\partial^2 C_u}{\partial z^2}=D_z^*\frac{\partial^2 C_u}{\partial z^2}-K_E\frac{1}{A\bar{\epsilon}_l}(C_u-C_d) \tag{37}$$

$$\frac{\partial C_d}{\partial t}-U_d\frac{\partial^2 C_d}{\partial z^2}=D_z^*\frac{\partial^2 C_d}{\partial z^2}+K_E\frac{1}{A\bar{\epsilon}_l}(C_u-C_d) \tag{38}$$

where, as before, we have taken equal flow areas for the two regions. We could have assigned different liquid fractions to the two regions, as did Anderson and Rice (1989), but this only complicates the issue. Thus, relative to the previous case, the present circumstance suggests equality of interstitial velocities, $U_u=U_d$, which is not at variance with equality of superficial velocities, $V_u=V_w$, since a uniform, average liquid fraction is used.

If we add the two equations, noting for batch conditions that the magnitudes of velocity are equal, $U_u=U_d=U$, we find:

$$\frac{\partial(C_u+C_d)}{\partial t}+U\frac{\partial(C_u-C_d)}{\partial z}=D_z^*\frac{\partial^2(C_u+C_d)}{\partial z^2} \tag{39}$$

Since we aim to reach a Fickian-like relationship, we shall need to designate a composition average across the column cross-section, so since flow areas are equal, then define:

$$\overline{C}=\frac{C_u+C_d}{2} \tag{40}$$

hence, Eq. 39 becomes:

$$\frac{\partial\overline{C}}{\partial t}+U\frac{\partial}{\partial z}\frac{(C_u-C_d)}{2}=D_z^*\frac{\partial^2\overline{C}}{\partial z^2} \tag{41}$$

Next, subtract Eq. 38 from Eq. 39 to see:

$$\frac{\partial(C_u-C_d)}{\partial t}+U\frac{\partial(C_u+C_d)}{\partial z}=D_z^*\frac{\partial^2(C_u-C_d)}{\partial z^2}$$

$$-\frac{2K_E}{A\bar{\epsilon}_l}(C_u-C_d) \tag{42}$$

But, we showed earlier that large exchange coefficients are likely, so $C_u\sim C_d$, and to a good approximation we conclude:

$$U\frac{\partial(C_u+C_d)}{\partial z}\simeq-\frac{2K_E}{A\bar{\epsilon}_l}(C_u-C_d) \tag{43}$$

Dividing by 2 and replacing $\overline{C}=(C_u+C_d)/2$ gives:

$$U\frac{\partial\overline{C}}{\partial z}\simeq-\frac{K_E}{A\bar{\epsilon}_l}(C_u-C_d) \tag{44}$$

Inserting this into Eq. 46 and collecting terms yields:

$$\frac{\partial\overline{C}}{\partial t}=\left[D_z^*+\frac{U^2A\bar{\epsilon}_l}{K_E}\right]\frac{\partial^2\overline{C}}{\partial z^2}=D_e\frac{\partial^2\overline{C}}{\partial z^2} \tag{45}$$

which is the sought after Fickian-Form where we have defined the effective dispersivity as:

$$D_e=D_z^*+\frac{U^2A\bar{\epsilon}_l}{K_E} \tag{46}$$

Again, the effective dispersivity takes a form analogous to Taylor diffusion, if we take $K_E\sim D_r^*$. Large circulation leads to large amplification of effective dispersivity. However, if the radial exchange coefficient is also large, the influence of circulation is diminished. The circulation model of Geary and Rice (1992) showed that circulation intensity increases as gas voidage increases (which is the same as superficial gas velocity

increasing), so U should increase (to a limit) as gas injection rate increases. Measurements which show D_e to be independent of gas rate may imply, according to the present model, that K_E swamps out effects arising from increases in U^2. This seems to be the case in the present experiments, as we show later.

The mathematical arguments for the simplified model described above was apparently first put forth as an "entrainment" model by Rietema some time ago (1982), for a different problem altogether (that is, mixing caused by entrainment in bubble wakes). In fact, the "entrainment" mechanism is identical in form to the convective part in Eq. 46 except for multiplication by a term α^2, where α was defined by Rietema as the fraction of liquid (continuous) phase which is entrained by rising bubbles. Thus, if entrainment is small (as with small, spherical bubbles), this mechanism contributes nothing to dispersivity. Moreover, the velocity in the present structure is circulation velocity, while in Rietema's entrainment model, it was slip velocity (which is the interstitial velocity of gas relative to liquid).

It is also noteworthy that some recent heat-tracer data (Lubbert et al., 1990; Lubbert and Larson, 1990) gave dispersion coefficients so dominated by convection that the authors concluded that the dominant mixing mechanism was due to transport by bubble wakes. As we saw in the previous development, liquid circulation produces an identical convective-dominated dispersion effect without invoking the very large, and physically unrealizable (and apparently unmeasurable) phenomenon of huge entrainment in bubble wakes. It remains to be proved that an entrainment mode can cause the large dispersion coefficients reported in literature. On the other hand, it is now quite well established (both by measurement and theory) that circulation often exists, in columns sparged by perforated plates. Both of the models discussed here fall in the category of *Taylor dispersion*, since they show the connection between axial convectio.ı and radial diffusion which leads to an effective enhancement of axial mixing (dispersion).

Experimental Methods

In this section, we discuss the methods and techniques used to deduce the sought after physical parameters. We discuss transient dispersion first, since data obtained from these experiments produce the needed values of entrance (CSTR) height, to be used in the steady-state experiments.

Acid-Base Neutralization Technique

The basis for the batch acid-base technique is to set up two chemically different regions in a column, which are driven by Fickian-like concentration gradients, as explained by Rice and Littlefield (1987). Thus, the liquid phase of bubble column is comprised of dilute acid (containing an indicator such as phenolphthalein) and alkali is slowly pumped into the bottom of the operating bubble column. A moving boundary forms which separates the upper acid region (colorless) from the lower base region (pink). As we have previously shown (Littlefield and Rice, 1987; Rice et al., 1990), a VCR recording of the upward movement of the moving boundary allows the entrance height and dispersion coefficient to be found. The solution of Eq. 45 for these conditions was given as:

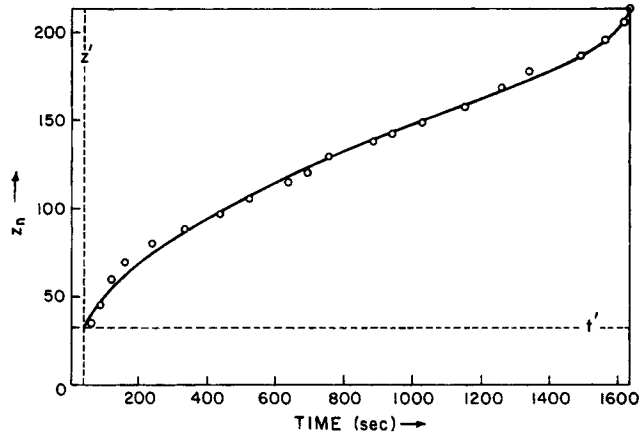

Figure 2. Movement of line of neutralization (z_n, cm) for 12 mPa·s solution of CMC at $U_{og}=1$ cm/s; $D_e=2.48$ cm²/s, $H=32.6$ cm, $t_n^*=38.8$ s.

$$\frac{C_{Ao}(1-\bar{\epsilon})D_e}{LN_B}=-\frac{z_n}{L}+\frac{1}{3}+\frac{D_e t_n}{L^2}+\frac{z_n^2}{2L^2}-\frac{2}{\pi^2}\sum_{m=1}^{\infty}\frac{\cos(m\pi z_n/L)}{m^2}\exp\left(\frac{-m^2\pi^2 D_e t_n}{L^2}\right) \quad (47)$$

The dispersivity (D_e) is fitted to the position, time data (z_n, t_n) corresponding to the moving "neutralization" boundary. In the early time periods, up to ten of the summation terms are necessary. However, for very large times, corresponding to the time to neutralize column contents (τ_{mix}) at $z_n=L$, the summation terms are often small and dispersion is approximately related to mixing time as follows:

$$\tau_{\text{mix}}\cong\frac{L^2}{6D_e}+\frac{n_{Ao}}{qC_{Bo}} \quad (48)$$

where n_{Ao} is the total acid initially present (moles) and qC_{Bo} is the rate of alkali added (mol/s). The circulation theory of Geary and Rice (1992) predicted $\tau_{\text{mix}}^{-1}\propto\sqrt{\epsilon}$.

By fitting Eq. 47 in a detailed way to distance-time data, both CSTR height (H) and D_e can be obtained. Thus, the Fickian zone starts somewhat up from the column base, so we replace coordinates in Eq. 47 with

$$z_n'=z_n-H;\quad t_n'=t_n-t_n^* \quad (49)$$

where H is the CSTR height and t_n^* is the time necessary to neutralize acid in the CSTR zone; this routine insures the Fickian zone begins at $z_n'=0$, $t_n'=0$, as illustrated by an actual set of data in Figure 2. A least-squares routine was used to find the best fit values for H and D_e, as described elsewhere (Rice, Barbe and Geary, 1990; Geary, 1991). It is important to note that D_e values are strictly applicable only to the smooth bubbly zone well *above* the entrance, so these values will not be inflated by chaotic events at the entrance region.

Analysis of Dispersion Data

The results of the experiments on a column 0.14 m ID and

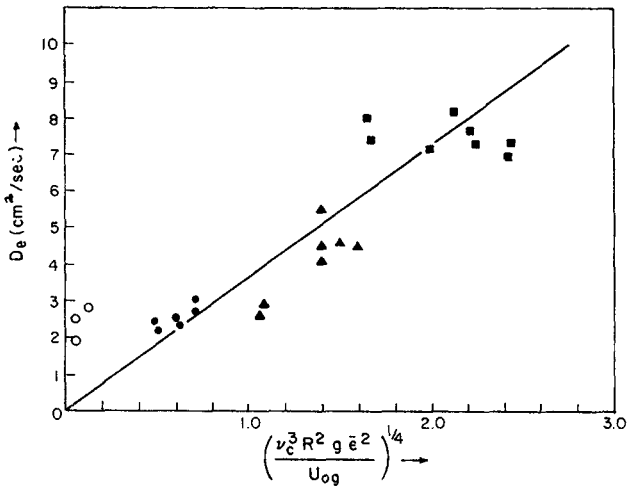

Figure 3. Parity plot for predicted eddy diffusivity (Eq. 54); ○ = 1, ● = 12, ▲ = 25, and ■ = 50 mPa·s solutions.

2.5 m high for varying viscosity are summarized in Figure 3. We remark that the column used was precisely vertical, adjustments being made using a spring-loaded micrometer system described elsewhere (Barbe, 1989; Rice et al., 1990; Geary, 1991). The gas sparger was a rubber sheet of 100 mm diameter, made of 3 mm thick latex which had 110 drilled holes on a triangular pitch; the holes were drilled with a 0.387 mm drill bit yielding a photographed hole size 0.138 mm. Details of the dynamics of bubble formation from this sparger have already been published (Geary and Rice, 1991). Suffice to say, predicted bubble diameter based on formation dynamics were matched very closely by photographed sizes.

For higher viscosity, the data tabulated in Geary (1991) suggest:

$$D_e \propto \mu^{0.75} \tag{50}$$

Such strong dependence on viscosity has not heretofore been observed. Deckwer et al. (1982), using similar CMC solutions, observed that D_e increased as CMC concentration increased, but a correlation with viscosity was not made (concentrated CMC solutions generally behave as power law fluids). Since the dispersivity was so small, varying from a low of 1.9 to a high value of 8.5 cm³/s, one might conclude that the Taylor contribution arising from the term containing U^2/K_E must be quite small, since Geary and Rice (1992) demonstrated that circulation velocity varies as $\sqrt{\epsilon}$, so U^2 should change significantly as U_{og} increases (unless K_E changes in the same way). We emphasize the two distinct features of the present experimental conditions:

1. Perfect verticality was strictly maintained.
2. A highly uniform gas injection device (elastic sparger) was used, leading to very uniform voidage distribution.

The very small magnitude of measured dispersion coefficient, and the strong viscosity dependence, combine to suggest that liquid circulation probably exists but the rate is quite small for the present arrangement. Attempts were made to measure velocity in water columns sparged with the Flexisparger, using constant temperature anemometer (CTA), but only very small velocities were detected (a maximum of 5 cm/s at the centerline). Under such conditions the effective dispersivity approximates to the eddy dispersion coefficient. Moreover, if the turbulence is nearly isotropic, as we suspect in the current situation, then $D_z^* \simeq D_r^* = D^*$.

To obtain such a strong viscosity dependence, the scale for turbulence must be quite small. It is has been demonstrated using the Geary and Rice (1992) model and the recent radioactive tracer data of Devanathan et al. (1990) that local eddy diffusivity can be estimated using:

$$D^*(\xi) \simeq \nu^* = l(\xi) \cdot \sqrt{R g \bar{\epsilon}} \left(\frac{\xi \left[1 - \left(\frac{\xi}{\lambda} \right)^m \right]}{m \lambda^2} \right)^{1/2} \tag{51}$$

where the length scale l lies in the range $l_d \leq l \leq 2R$, and λ denotes the dimensionless position of maximum downflow velocity. Our 1992 work also showed that circulation velocity was only weakly affected by molecular viscosity owing to the large values of eddy viscosity computed. Thus, to realize the strong viscosity dependence obtained for the present data, we conclude the smallest possible eddy (that is, the Kolmogoroff diffusive scale) must be dominant in present conditions:

$$l_d \sim \left(\frac{\nu_c^3}{P_m} \right)^{1/4} \tag{52}$$

which would yield the observed 0.75 power on viscosity that exactly matches present data.

Since the parameter λ changes little with flow conditions ($\lambda \sim 1$), we can write the average for Eq. 51 the approximate result:

$$D^* = \frac{K \nu_c^{.75} \sqrt{R g \bar{\epsilon}}}{P_m^{1/4}} \tag{53}$$

where K is an arbitrary constant. If the total energy rate dissipated per unit mass is taken to be $P_m \simeq U_{og} \cdot g$ as suggested by Baird and Rice (1975), then eddy diffusivity for low circulation rates can be represented by:

$$D^* = k \left(\frac{\nu_c^3 R^2 g \bar{\epsilon}^2}{U_{og}} \right)^{1/4} \tag{54}$$

The data from Geary (1991) shown in Figure 3 indicate $K \simeq 3.6$; the semi-empirical result in Eq. 54 seems to correlate the data quite well. Gas velocity appears to have very little affect on dispersivity owing to the appearance of the ratio $\bar{\epsilon}^2/U_{og}$.

The relatively low magnitude of dispersivity, along with strong proportionality to viscosity, suggest that eddy diffusivity controls mixing in the current Flexisparged column. This finding does not reject the existence of circulation; indeed, some modest circulation must exist in order for D^* to be finite according to Eq. 51. However, we may infer that voidage profile is relatively uniform and that the voidage exponent m tends to be quite large. To an order of magnitude (see Geary and Rice, 1992), we can write $U_c \propto 1/l$ and $K_E \sim D_r^* R/l$, so that $U_c^2/K_E \propto 1/l$. Had we taken $l = l_d$, the Taylor contribution would give the inverse of viscosity dependence relative to present

experiments. Had we taken $l \sim d$ (bubble diameter), then according to experiments using Flexisparger (Geary and Rice, 1991), photographed values of d corresponded to formation size at the sparger head. The dynamics of formation size was such that roughly $d \propto \mu^{1/4}$, so again, an incorrect, inverse viscosity dependence would have arisen from the Taylor contribution, and as well in the eddy term. Finally, if we assumed that the "entrainment" model explained mixing, then D_e would be proportional to the square of slip velocity U_s. According to the Richardson-Zaki expression, slip velocity is proportional to terminal rise velocity which in turn is proportional to $\mu^{-1/3}$ according to Rice and Littlefield (1987). Again, we arrive at an incorrect (inverse) viscosity dependence.

Thus, after exhausting all possible models and mechanisms, only one yielded the correct viscosity dependence, and also gave values within an order of magnitude of measured dispersivity. The data in Figure 3, and the structure of the model in Eq. 46, suggest that an asymptote may exist when the group $(\nu_c^3 R^2 g \bar{\epsilon}^2 / U_{og})^{1/4}$ becomes small (~ 1 cm^2/s). Detailed measurements, of the type conducted by Lubbert and coworkers (1990), may shed light on values for locally varying D_r^* and D_z^*. These measurements, combined with Eq. 46, may explain the curious behavior patterns and property dependences of bubble columns. It is now becoming clear that formerly ignored installation details (column verticality, sparger properties) play a key role in column dynamics. At this point, it now appears certain that the size and shape of radial voidage distribution is the primordial engine for column dynamics. The origin for such distributions, and its relation to physical-chemical properties of the phases, has yet to be uncovered.

Finally, we also obtained estimates of the height of the entrance region, which was fitted to a simple linear relation as follows:

$$H = 0.87 - 7.31\bar{\epsilon} \text{ (m)} \tag{55}$$

This height steadily diminishes as gas velocity increases. This behavior can be rationalized as follows. The chaotic entrance region behaves somewhat like the churn-turbulence regime, giving way to a smooth bubbly flow pattern somewhat upward away from the entrance. At higher gas velocities, the entire column operates in the churn-turbulence regime so at voidages greater than around 10%, there exists no smooth bubbly region and the entire column behaves according to the churn-turbulence pattern; so, for such cases the entrance zone no longer exists.

Parameter Estimation for Gas Absorption Experiments

Arguments arising from measurement of dispersivity suggest circulation in the current arrangement is quite small, as verified by CTA measurement, so the asymptotic result from Eq. 32 can be used to model local mass transfer:

$$\frac{C(z) - C^*}{C_o - C^*} \simeq \frac{1}{1 + \dfrac{k_c^* a H}{U_o}} \exp\left(- \frac{K_L a \cdot z}{2U_o} \right) \tag{56}$$

The absolute length scale measured from the column base is $z'' = z + H$, where z was the scale commencing the bubbly zone.

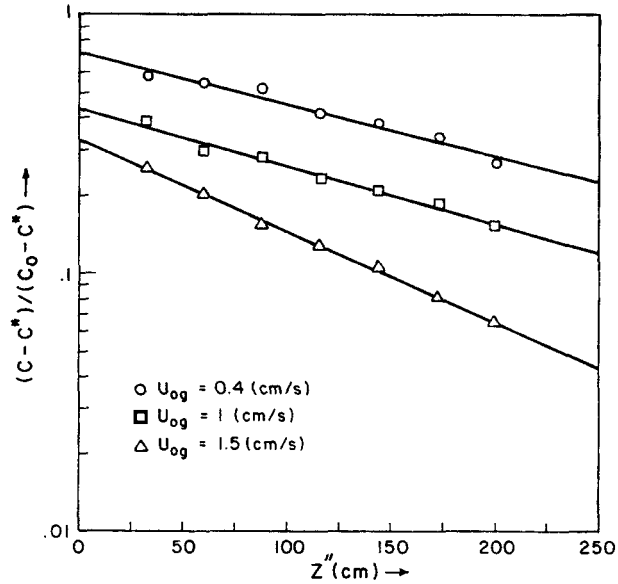

Figure 4. Dissolved oxygen profiles for 12 mPa·s CMC solution; $U_o = 1.5$ cm/s.

Dissolved oxygen probes were placed at positions (measured from the base): 33, 60, 88, 116, 144, 173 and 200 cm. It is convenient to use the absolute scale, so we replace $z = z'' - H$, and recall that $K_L a = k_c a(1+\alpha)$, so Eq. 56 takes the form:

$$\frac{C(z) - C^*}{C_o - C^*} = \frac{\exp\left[\dfrac{H k_c a(1+\alpha)}{2U_o} \right]}{1 + \dfrac{k_c^* a H}{U_o}} \exp\left[- \frac{k_c a(1+\alpha) z''}{2U_o} \right] \tag{57}$$

which could be used to estimate $k_c a(1+\alpha)$ and $k_c^* a$, since H is known from independent transient dispersion experiments. On semi-log paper, the slope yields $k_c a(1+\alpha)$, while the intercept allow estimates of $k_c^* a$. Typical fits of the data are shown in Figure 4. Using the present center-line measurements, it is not possible to independently deduce values for α, but arguments given earlier suggest $\alpha \simeq 1$, which is the plug-flow (large exchange coefficient, K_E) case.

Dissolved oxygen was measured along the column centerline. The dissolved-oxygen meter (YSI Model 57) was attached to a probe which uses a Clark-type membrane covering polarographic sensor with built in thermisters for temperature measurement and compensation. The probe (YSI model 5739) was inserted into a well-stirred flask through which liquid samples were drawn from sample ports along the column length. Mass flow of pure oxygen was monitored by a solid-state mass flow meter (STEC SEF-1454). Additional details of column and ancillary equipment can be found in the thesis of Geary (1991).

Analysis of Absorption Rates

The entrance region for the present system was modeled as a CSTR, which implies well-mixed behavior. In fact, more can be said about behavior at the entrance, relative to standard definitions of bubble column flow regimes. In all cases, the flow pattern at the entrance behaved in a chaotic pattern like

the churn-turbulence regime, gradually giving way to a smooth bubbly-flow pattern a short distance upward. Thus, at the entrance, surface renewal is quite fast and turbulence appears everywhere isotropic. Under such conditions, we may modify the penetration model for average transport coefficient at the entrance, that is:

$$k_c^* = \sqrt{\frac{4D}{\pi t_e^*}} \tag{58}$$

by expressing exposure time using a time scale based on Kolmogoroff's length and velocity, as apparently first suggested by Kastanek (1977). We can write within an arbitrary constant, the result:

$$t_e^* \sim v^*/l_d = (P_m \nu)^{1/4}/[\nu^{.75}/P_m^{1/4}] \tag{59}$$

For spherical bubbles, the interfacial area per unit volume emulsion is $a = (6/d)\bar{\epsilon}$, so under conditions of isotropic turbulence, Eqs. 58 and 59 are combined with area to yield:

$$k_c^* a = 6\sqrt{\frac{4D}{\pi}}\left(\frac{P_m}{\nu}\right)^{1/4}\left(\frac{\bar{\epsilon}}{d}\right) \tag{60}$$

Replacing $P_m \cong U_{og} \cdot g$, the Kolmogoroff scaled volumetric transport coefficient is:

$$k_c^* a = 6\sqrt{\frac{4}{\pi} D}\left(\frac{U_{og} g}{\nu}\right)^{1/4}\left(\frac{\bar{\epsilon}}{d}\right) \tag{61}$$

In the limit for increasing gas velocity, the upper regions of the column may also obey the Kolmogoroff scaling, in light of the results for dispersion coefficient discussed earlier. We shall compare predictions from Eq. 61 with both $k_c^* a$ and $k_c a$ data.

Results for four different viscosities are compared with predictions from Eq. 61 in Figures 5 and 6. It is seen, within an arbitrary multiplicative constant, that the Kolmogoroff scaling seems to track data for $k_c^* a$ and $k_c a$. Thus, as expected, $k_c^* a$ follows a line which is a factor 4 larger than predicted from Eq. 61, while $k_c a$ is about one-half the magnitude predicted by that equation. For the medium range CMC (ICN Biochemicals, molecular weight ~250,000) in the low concentrations used here (< 1 wt. %), Yagi and Yoshida (1975) reported that oxygen diffusivities were essentially unchanged from that of water at 25°C, so a value of 2.3×10^{-9} m^2/s was used for all cases. A Brookfield plate-cone viscometer was used to check Newtonian behavior for all the large batches of solutions, and also to insure quality control, so that measured viscosities had error bounds: 12 ± 1, 25 ± 1, and 50 ± 3 mPa·s. Bubble size was calculated using the formation dynamics published earlier (Geary and Rice, 1991) for the same sparger and viscosities used here. Photographic evidence (Image analysis) showed formation size was almost identical to calculated values. This size was also verified independently (Geary, 1991) using the chemical method.

Voidage was determined using the standpipe method, on batch columns, and this was correlated using the Richardson-

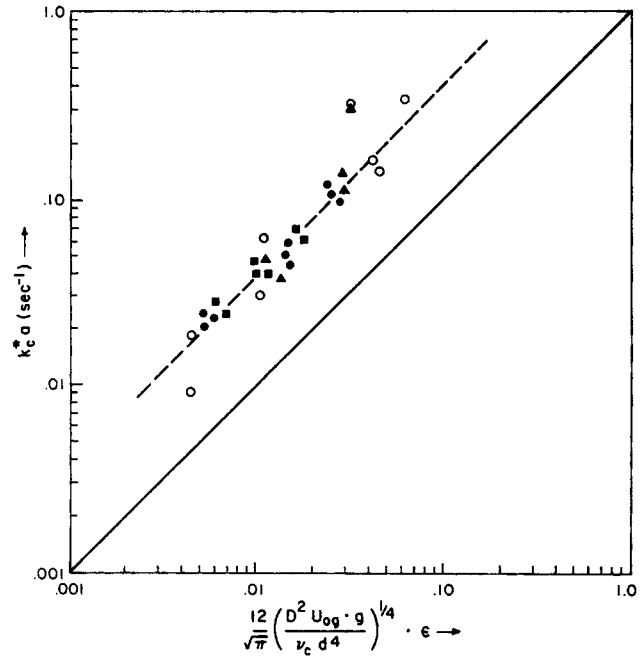

Figure 5. Comparison of entrance zone transfer coefficient with Kolmogoroff scaled predictions (Eq. 61); ○ = 1, ● = 12, ▲ = 25 and ■ = 50 mPa·s solutions.

Zaki definition of slip velocity, where ϵ now represents mean voidage:

$$U_s = U_t(1-\epsilon)^{n-1} = \frac{U_{og}}{\epsilon} \tag{62}$$

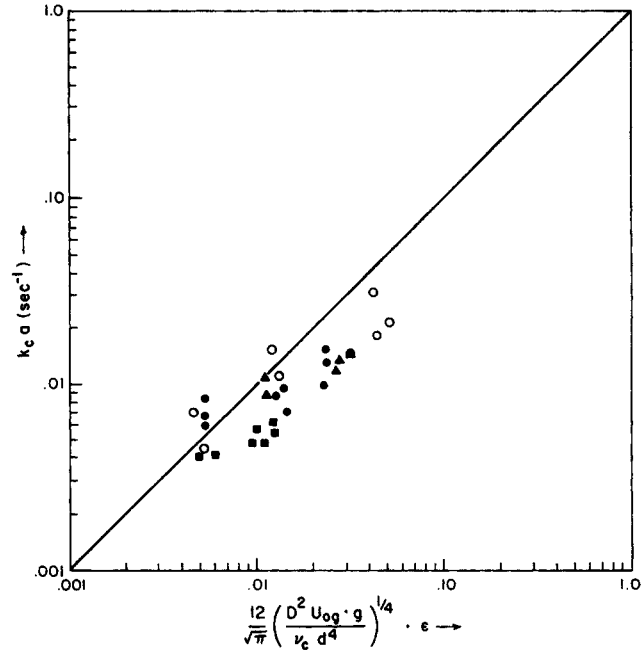

Figure 6. Comparison of bubbly zone transfer coefficients with Kolmogoroff scaled predictions (Eq. 61); ○ = 1, ● = 12, ▲ = 25 and ■ = 50 mPa·s solutions.

Table 1. Effect of Viscosity on Richardson-Zaki Parameters and Transition Velocity (Geary, 1991)

Viscosity mPa·s (cp)	Transition U_{og} cm/s	Parameter Fitted	
		U_t cm/s	n
1	3	27.5	3
12	2.5	26.5	3
25	2.5	18.85	3
50	1.5	15.5	3

which is applicable only to noncirculating systems. Geary (1991) has provided an analytical correction to this to account for circulation. For all the systems studied, the coefficient n took a best-fit value of 3. The fitted values for terminal rise velocity as a function of viscosity are shown in Table 1 along with the magnitude of superficial gas velocity at the onset of transition to churn-turbulent flow conditions. Voidages for cocurrent absorption experiments were determined from known values of U_t and n using the two-phase flow relative velocity:

$$U_t(1-\epsilon)^2=\frac{U_{og}}{\epsilon}-\frac{U_o}{1-\epsilon} \tag{63}$$

which can be rearranged to solve for ϵ by graphical means using the form:

$$U_t\epsilon(1-\epsilon)^3=U_{og}-\epsilon(U_{og}+U_o) \tag{64}$$

as suggested by Wallis (1969). Thus, ϵ is deduced by finding the intersection of the nonlinear LHS with the linear RHS. It was necessary to calculate voidage in this way owing to the physical arrangement of the co-current absorption experiment. Thus, a closed system was used so that mass-flow meters at entrance and exit could be used as a double-check on the rate of oxygen uptake. In-line dryers for these mass-flow meters elevated exit gas pressure, so it was necessary to disconnect the standpipe used in the batch columns. Voidages calculated in this way were less than around 10% for the data reported in Figures 5 and 6.

Comments and Conclusions

It is now becoming evident (Rice et al., 1981, 1990; Deckwer et al., 1982; Rice and Littlefield, 1987; Geary and Rice, 1991) that the Flexisparger (elastic membrane sparger) has unique properties which produce highly uniform conditions leading to nearly ideal bubbly flow. Thus, under conditions of perfect vertical alignment, it has been demonstrated that bubble columns can be operated with minimum global circulation leading to low measured values of axial dispersion coefficient. This coefficient is so low, it can safely be ignored in the design exercise. Moreover, it has been reported by others (Dekwer et al., 1982), and the present work provides verification, that the Flexisparger produces maximum volumetric transfer coefficients, even for viscous solutions.

We have also produced, apparently for the first time, models which allow for elementary corrections to the plug-flow case for conditions when entrance zone effects are significant, and also when circulation is large and when radial dispersion is poor. The latter corrections are shown to be unnecessary when optimum sparging is used in the first instance. However, there are viable process conditions which mandate significant circulation, for example, to maintain suspension in slurry reactors. For such cases, it is suggested that columns should be slightly tilted, and that center-mounted single-hole nozzles be used for gas sparging, unlike the present case wherein uniform gas injection by Flexisparger practically eliminates circulation.

Finally, we conclude that Kolmogeroff scaling leads to the correct order of magnitude for bubble contact time in application of the penetration theory to compute transfer coefficients. This model has the penalty that good bubble size estimates are necessary for proper design. The problem of breakage and coalesence under practical conditions has not been resolved, so estimating bubble size is not a trivial matter.

While the full extent of the circulation models presented have not been experimentally tested, owing to the small column diameter used and the well-behaved properties concomitant to the Flexisparger, nonetheless, the models may be useful to practioneers who are forced by circumstance to use standard spargers, such as perforated plates and ring spargers in large diameter columns. It is clear that the mode of gas injection has significant effects on the liquid flow pattern upstream, and a circulatory flow pattern can reduce mass transfer, increase dispersion and also reduce gas contact time by short-circuiting.

Notation

a = interfacial area per unit volume emulsion, m^2/m^3
A = one-half column cross-sectional area, m^2
A_o = full column cross-sectional area, m^2
A_u = upflow cross-sectional area, m^2
A_d = downflow cross-sectional area, m^2
C = liquid composition in CSTR zone, mol/m^3
C^* = solubility dissolved oxygen, mol/m^3
C_d = liquid downflow composition, mol/m^3
C_o = liquid inlet composition, mol/m^3
C_u = liquid upflow composition, mol/m^3
d = bubble diameter, m
D = Heaviside operator, or molecular diffusion, m^2/s
D^* = eddy diffusion coefficient, m^2/s
D_e = effective dispersion coefficient, m^2/s
H = height of CSTR zone, m
k_c^*a = volumetric mass-transfer coefficient in CSTR zone, s^{-1}
k_ca = volumetric mass-transfer coefficient in bubbly zone, s^{-1}
K_E = radial exchange coefficient, m^2/s
l = eddy mixing length scale, m
l_d = Kolmogoroff eddy scale, m
L = emulsion height, m
m = exponent for radial voidage distribution
N_B = flux of alkali added, $mol/m^2 \cdot s$
n = Richardson-Zaki exponent
n_{Ao} = total moles acid present initially, mol
P_m = rate of energy input per unit mass, m^2/s^2
q = volume flow alkali, m^3/s
q_d = dimensionless downflow rate, Q_d/Q_o
q_u = dimensionless upflow rate, Q_u/Q_o
Q_d = volume rate downflow liquid, m^3/s
Q_o = volume rate liquid flow, m^3/s
Q_u = volume rate upflow liquid, m^3/s
R = column radius, m
U = interstitial liquid velocity, m/s
U_o = superficial liquid velocity, m/s
U_{og} = superficial gas velocity, m/s
U_t = terminal rise velocity of bubble, m/s
z = axial coordinate from bottom, m
z_n' = coordinate beginning Fickian Zone in acid-base experiment, m
z_n'' = actual distance from column base in absorption experiment, m

Greek letters

α = dimensionless coefficient $[K_E/(K_E+k_caA)]$
δ = velocity inversion position, dimensionless
ϵ = gas volume fraction
ϵ_l = liquid volume fraction
ζ = dimensionless length scale, $z(k_caA+K_E)/Q_o$
θ_d = C_d-C^*, downflow concentration difference, mol/m^3
θ_u = C_u-C^*, upflow concentration difference, mol/m^3
μ = liquid viscosity, mPa·s
ν = kinematic liquid viscosity, m^2/s
ξ = dimensionless radial coordinate

Literature Cited

Anderson, K. G., and R. G. Rice, "Local Turbulence Model for Predicting Circulation Rates in Bubble Columns," *AIChE J.*, **35**, 514 (1989).

Baird, M. H. I., and R. G. Rice, "Axial Dispersion in Large Unbaffled Columns," *Chem. Eng. J.*, **9**, 171 (1975).

Barbe, D. T., "Mixing Phenomena in Tilted Bubble Columns," MS Thesis, LSU (1989).

Clark, N. N., C. M. Atkinson, and R. L. C. Flemmer, "Turbulent Circulation in Bubble Columns," *AIChE J.*, **33**, 515 (1987).

Deckwer, W. D., A. Schumpe, K. Nguyen-Tien, and Y. Serpemen, "Oxygen Mass Transfer into Aerated CMC Solutions in a Bubble Column," *Biotech. and Bioeng.*, **24**, 461 (1982).

Devanathan, N., D. Moslemian, and M. P. Dudukovic, "Flow Mapping in Bubble Columns Using CARPT," *Chem. Eng. Sci.*, **45**, 2285 (1990).

Geary, N. W., and R. G. Rice, "Bubble Size Prediction for Rigid and Flexible Spargers," *AIChE J.*, **37**, 161 (1991).

Geary, N. W., "On Bubble Columns," PhD Thesis, Louisiana State University (1991).

Geary, N. W., and R. G. Rice, "Circulation and Scale-up in Bubble Columns," *AIChE J.*, **38**, 76 (1992).

Kastanek, F., "The Volume Mass Transfer Coefficient in a Bubble Bed Column," *Coll. Czech. Chem. Commun.*, **42**, 2491 (1977).

Kojima, E., H. Unno, Y. Sato, T. Chida, H. Imai, K. Endo, I. Inque, J. Kobayashi, H. Kaji, H. Nakanishi, and K. Yamamoto, "Liquid Phase Velocity in 5.5 m Diameter Bubble Column," *J. Chem. Eng. Japan*, **13**, 16 (1980).

Lubbert, A., and B. Larson, "Detailed Investigation of the Multiphase Flow in Airlift Tower Loop Reactors," *Chem. Eng. Sci.*, **45**, 3047 (1990).

Lubbert, A., B. Larson, and S. Broring, "Local Mixing Behavior of Airlift Multiphase Chemical Reactors," *Int. Chem. Eng. Symp. Ser.*, 121 (1990).

Rice, R. G., D. T. Barbe, and N. W. Geary, "Correlation of Non-Verticality and Entrance Effects in Bubble Columns," *AIChE J.*, **36**, 1421 (1990).

Rice, R. G., and M. Littlefield, "Dispersion Coefficients for Ideal Bubbly Flow in Truly Vertical Bubble Columns," *Chem. Eng. Sci.*, **42**, 2045 (1987).

Rice, R. G., and N. W. Geary, "Prediction of Liquid Circulation in Viscous Bubble Columns," *AIChE J.*, **36**, 1339 (1990).

Rietema, K., "Science and Technology of Dispersed Two-Phase Systems: I & II," *Chem. Eng. Sci.*, **37**, 1125 (1982).

Wallis, G. B., *One Dimensional Two-Phase Flow*, McGraw-Hill, New York (1969).

Wilkinson, P. M., "Physical Aspects and Scale-Up of High Pressure Bubble Columns," PhD Thesis, University of Groningen, The Netherlands (1991).

Yagi, H., and F. Yoshida, "Gas Absorption by Newtonian and Non-Newtonian Fluids in Sparged, Agitated Vessels," *Ind. Eng. Chem., Process Des. Dev.*, **14**, 488 (1975).

Manuscript received June 2, 1992, and revision received Aug. 28, 1992.